

Dynamic Allan variance analysis for stochastic errors of fiber optic gyroscope

Zhang Chunxi¹, Wang Lu¹, Gao Shuang¹, Li Huipeng¹, Lin Tie¹, Li Xianmu¹, Wang Tao²

- (1. School of Instrumentation Science and Opto-electronics Engineering, Beihang University, Beijing 100191, China;
2. Beijing Aerospace Times Laser Navigation Technology Limited Liability Company, Beijing 100094, China)

Abstract: In allusion that classical Allan variance cannot highlight the nonstationary of stochastic errors of Fiber Optical Gyroscope (FOG), and Dynamic Allan Variance (DAVAR) can, but there was no theory which proved the validity and the effectiveness of DAVAR systematically. The DAVAR, a measure of the time-varying stability of FOG was presented and discussed. First, the classical Allan variance and DAVAR were mathematically defined, and then their behaviors were extensively tested on simulated and experimental FOG output signal. What's more, FOG stochastic errors changes were quantitatively described by a two-dimensional method. Results prove the validity and effectiveness of the proposed new tool using for analyzing the stochastic errors of FOG. DAVAR analysis method not only can determine the coefficients of FOG stochastic error, but also can describe their non-stationary. DAVAR is a more comprehensive, more effective and more useful tool for judging FOG performance.

Key words: FOG; random error; Allan variance; DAVAR

CLC Number: TN253 **Document code:** A **Article ID:** 1007-2276(2014)09-3081-08

基于动态 Allan 方差的光纤陀螺随机误差分析

张春熹¹, 王璐¹, 高爽¹, 李慧鹏¹, 林铁¹, 李先慕¹, 王涛²

- (1. 北京航空航天大学 仪器科学与光电工程学院, 北京 100191;
2. 北京航天时代激光导航技术有限责任公司, 北京 100094)

摘要: 针对经典 Allan 方差不能反映光纤陀螺(FOG)随机误差的非平稳特性, 动态 Allan 方差(DAVAR)可以反映但没有理论系统地证明其正确性和有效性的问题, 通过仿真数据验证了 DAVAR 的正确性; 利用实验数据分析光纤陀螺噪声随时间变化的动态特性, 证明了 DAVAR 的有效性。首先, 阐述了经典 Allan 方差和动态 Allan 方差的数学定义, 然后利用仿真和实验数据验证其特征, 并实现了光纤陀螺噪声的定量二维描述。实验结果表明: DAVAR 不仅可以辨识和分离光纤陀螺随机误差, 还可以确定噪声系数, 更重要的是可以描述光纤陀螺随机信号动态特性。因此, DAVAR 是分析光纤陀螺特性更加全面、有效且实用的工具。

关键词: 光纤陀螺; 随机误差; Allan 方差; 动态 Allan 方差

收稿日期: 2014-01-19; 修订日期: 2014-02-20

作者简介: 张春熹(1965-), 男, 教授, 博士生导师, 主要从事光纤陀螺方面的研究。Email: zhangchunxi@buaa.edu.cn

通讯作者: 王璐(1988-), 女, 博士生, 主要从事光纤陀螺信号处理方面的研究。Email: wanglu@aspe.buaa.edu.cn

0 Introductions

Fiber Optic Gyroscope (FOG) has so many particular merits, such as high precision, impulsion resistance, shock resistance and wide measuring range that it has been widely applied to the aerospace field^[1]. The fundamental characteristics of an FOG are its stability and precision which influence its application. Allan variance is a time domain analysis method and a standard quantity for the characterization of oscillatory stability recommended by international standardizations organizations David Allan. Allan variance could characterize and identify the statistical characteristics of various error sources. Treating FOG output by Allan variance can analyze identify the inherent noise error^[2]. Therefore Allan variance is an important method for measuring and judging FOG's performance. However, classical Allan variance is effective just for ideal time-varying series, and the real time-varying series is non-stationary, even though between short time intervals. In long time, FOG is influenced by environmental factors such as temperature and humidity, and eventually age and break down like any physical device. Consequently, the stability of FOG varies with time. Therefore it is important to introduce a quantity that can represent the time-varying stability of the FOG. This paper presents the Dynamic Allan Variance (DAVAR), which defines the stability of a FOG as a function of time.

DAVAR was recommended by L. Galleani for measuring atomic clock stability. DAVAR is a new method for analyzing time series which can track and describe the nonstationary factors of signal^[3-7]. Wei Guo. etc put it in application to evaluating Ring Laser Gyro random error^[8]. Li Ying. etc applied it to FOG static data^[9]. Li Xuyou and Zhang Na. etc used it to analyze swing signal of marine FOG and researched on the influence of window function on DAVAR^[10-11]. But, no one fully prove DAVAR's correctness, validation and practicability, and no one realize a

two-dimensional quantitative description for the major noise coefficient of FOG drift signal. In order to verify DAVAR and analyze the properties of FOG noise more comprehensively, we analyze classical Allan variance and dynamic Allan variance comparatively by establishing three simulated data and an experimental data. The results show DAVAR's effectiveness and FOG random error nonstationary qualitatively, at the same time, this paper realize a two-dimensional quantitative description for the major noise coefficient of FOG stochastic errors.

1 Classic Allan variance

If the Allan variance is to be estimated on N discrete FOG samples $\Omega_n(t_0)$, where t_0 is the sampling period, then the time axis t is sampled as $t=nt_0$. Establishing array with k consecutive data and time length of array is $\tau=kt_0$; consequently, the t axis is discretized. Because $k=1,2,\dots,l(l<n/2)$, then can also be interpreted as the minimum observation interval. Then we calculate ensemble average of each array, that is

$$\bar{\Omega}_p(\tau)=\frac{1}{\tau}\int_{t_p}^{t_{p+\tau}}\Omega(t)dt\text{ or } \bar{\Omega}_p(\tau)=\frac{1}{k}\sum_{i=p}^{p+k}\Omega_i(t_0)\quad (1)$$

Which, in practice, is performed through a time average, under the assumption of ergodicity. The symbol $\bar{\Omega}_p(\tau)$ in Eq.(1) denotes group average of array which begins with p data points and time length is $\tau=kt_0$. Given τ will get $n-k+1$ group averages. Define the average difference between the adjacent arrays as

$$\xi_{p+1,p}=\bar{\Omega}_{p+1}(\tau)-\bar{\Omega}_p(\tau)\quad (2)$$

Then the Allan variance is defined as

$$\sigma^2(\tau)=\frac{1}{2(n-k-1)}\sum_{p=1}^{n-k-1}[\xi_{p+2,p+1}-\xi_{p+1,p}]^2=$$

$$\frac{1}{2(n-k-1)}\sum_{p=1}^{n-k-1}[\bar{\Omega}_{p+2}(\tau)-2\bar{\Omega}_{p+1}(\tau)+\bar{\Omega}_p(\tau)]^2\quad (3)$$

N, K, B, Q, R represent coefficients of the FOG five stochastic errors respectively, angular random

walk, rate random walk, bias instability, the quantization noise, the rate slope. Allan variance associated with the noise's power spectrum in the original data, and different types of random process can be tested by using different sampling times τ ^[3]. If keep the actual test environment stability, it can be considered that these error sources are statistically independent. At this time, Allan variance can be expressed as one or several error sources' variance square sum. Thus, it can be approximately defined as:

$$\sigma^2(\tau) = \sigma_{QN}^2(\tau) + \sigma_{ARW}^2(\tau) + \sigma_{BI}^2(\tau) + \sigma_{RRW}^2(\tau) + \sigma_{RR}^2(\tau) = \frac{3Q^2}{\tau^2} + \frac{N^2}{\tau} + \frac{2B^2}{\pi} \ln 2 + \frac{K^2 \tau}{3} + \frac{R^2 \tau^2}{2} \quad (4)$$

Organizing Eq.(4) get

$$\sigma^2(\tau) = \sum_{n=-2}^2 C_n \tau^n \quad (5)$$

Fitting the Allan variance curve by the least squares method can obtained the coefficients C_n . According to the corresponding coefficients are equal, the error coefficient derived as follows:

$$\begin{aligned} N &= \frac{\sqrt{C_{-1}}}{60} ((^\circ)/h)^{1/2} \\ K &= 60\sqrt{3C_1} ((^\circ)/h)^{3/2} \\ B &= \frac{\sqrt{C_0}}{0.664} ((^\circ)/h) \\ Q &= \frac{10^6 \pi \sqrt{C_{-2}}}{180 \times 3 \times 600 \times \sqrt{3}} (\mu\text{rad}) \\ R &= 3 \times 600 \sqrt{2C_2} ((^\circ)/h)^2 \end{aligned} \quad (6)$$

2 Dynamic Allan variance

DAVAR is improved and expanded of Allan variance. If we suspect that a FOG random signal has time-varying properties, we can repeat the evaluation of the Allan variance at different epochs. Then we collect all the variances obtained at every epoch, and we plot the result in single 3-D graph. This procedure corresponds to the definition of the DAVAR. The procedure can be summarized as follows:

- (1) Fix analysis time epoch t_1 ;
- (2) Define the window function $P_L(t')$ which length

is L and centered at t_1 ($t-L/2 \leq t_1 \leq t+L/2$). Truncate the FOG signal with $P_L(t')$. Consequently, we obtained truncated signal $y(t, t_1)$:

$$y(t, t_1) = x(t) P_L(t - t_1) \quad (7)$$

(3) Evaluate the Allan variance

$$\begin{aligned} \sigma^2(t_1, \tau) &= \frac{1}{2(N-k-1)} \sum_{p=1}^{N-k-1} [\xi_{p+2, p+1} - \xi_{p+1, p}]^2 = \\ &= \frac{1}{2(N-k-1)} \sum_{p=1}^{N-k-1} [\bar{\Omega}_{p+2}(\tau) - 2\bar{\Omega}_{p+1}(\tau) + \bar{\Omega}_p(\tau)]^2 \end{aligned} \quad (8)$$

(4) Choose another analysis epoch, say $t=t_2$, and repeat form step(2) and step(3). The new epoch t_2 can be chosen so that the corresponding truncated signal overlaps with the truncated signal related to the previous epoch t_1 .

At the end of the above procedure, the collection of variances $\sigma(t_m, \tau)$ (wherein $m=1, 2, \dots, K, K \leq n-m+1$) related to the M different epochs t_k and to the different observation intervals τ . Eventually we plot all the variances $\sigma(t_m, \tau)$ on the same 3-D graph according to the time sequence. Generally, the 3-D map uses the standard dynamic Allan deviation (dynamic Allan deviation, DADEV). That is $\sigma(t_m, \tau)$.

Then we propose an estimator for the DAVAR and test it on simulated and experimental data.

3 Simulation and experimental results

3.1 Simulation results

In this section, we apply the DAVAR to three simulated processes: $x_1(t)$ is stationary process, $x_2(t)$ and $x_3(t)$ are nonstationarities processes, but they are all uncorrelated and zero mean white Gaussian phase noise. Sampling time is 10ms, and time length is 10min, so total number of the simulated data is 60 000. Table 1 shows the character of simulated data.

Tab.1 Character of simulated data

Simulated data	Deviation
$x_1(t)$	$\sigma=1$
$x_2(t)$	Before 300 s $\sigma=1$, after 300 s $\sigma=2$
$x_3(t)$	$\sigma=1+(10/n) \times i$

Notation: n is the data's total number, and i is data epoch.

Figure 1 show the three groups simulated data.

The three sets of simulated data were analyzed by classical Allan variance and fitted with least squares method. The results were showed in Fig.2.

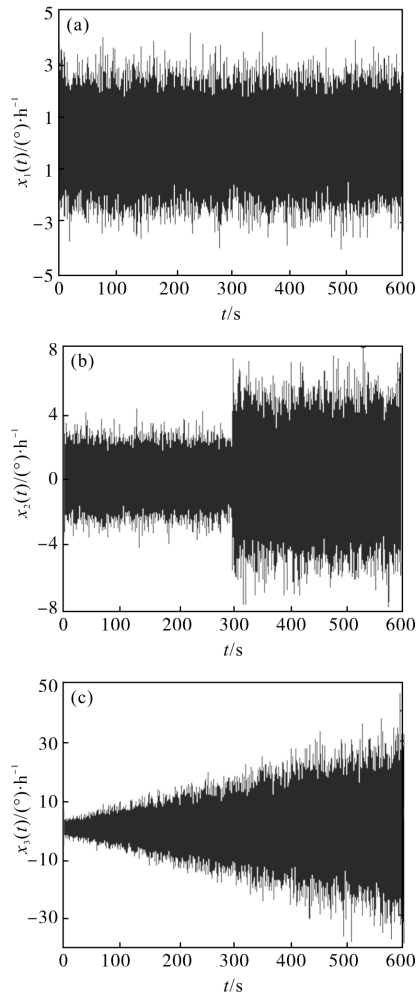


Fig.1 Three simulate data

$x_1(t)$ is stationary white Gaussian noise. It can be seen that, as expected, the Allan deviation has a slope proportional to $\tau^{-0.5}$, which indicates a white phase noise^[3]. $x_2(t)$ and $x_3(t)$ are non-stationary white noise, to our surprise, they both have a same constant slope of pure white phase noise with no evidence of the changing variance. Therefore the Allan deviation does not reveal the non-stationary of the processes.

Then we apply our method to the three groups of simulated data and compute their dynamic Allan deviation, which are shown in Fig.3. Truncation window is selected rectangle window whose length $L=$

900, and step length $L_0=300$.

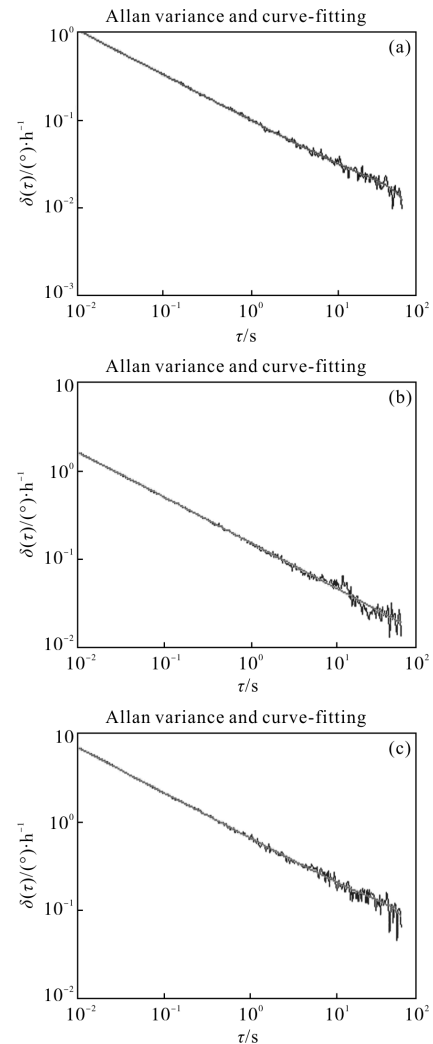


Fig.2 Simulate data corresponding Allan deviation

Because $x_1(t)$ is a stationary random process, it is expected also the instantaneous stability to be constant with time. This is precisely what happens, as can be noticed from Fig.3(a), where the dynamic Allan deviation (DADEV) is shown. The DADEV is constant with time and changes with τ only, with the typical slope of white phase noise and it has the same slope of the Allan deviation in Fig.2. $x_2(t)$ and $x_3(t)$ are non-stationary white noise, as expected, the DADEV highlight the presence of a non-stationary noise. From Fig.3(b), it can be inferred that $x_2(t)$ is composed by sequence of 2 stationary white phase noises. The transition happens in the middle of the signal. From Fig.3 (c), it can be seen that DADEV tracks the non-

stationary and highlights the changes in variance, it can be inferred that the signal's variance increase with time.

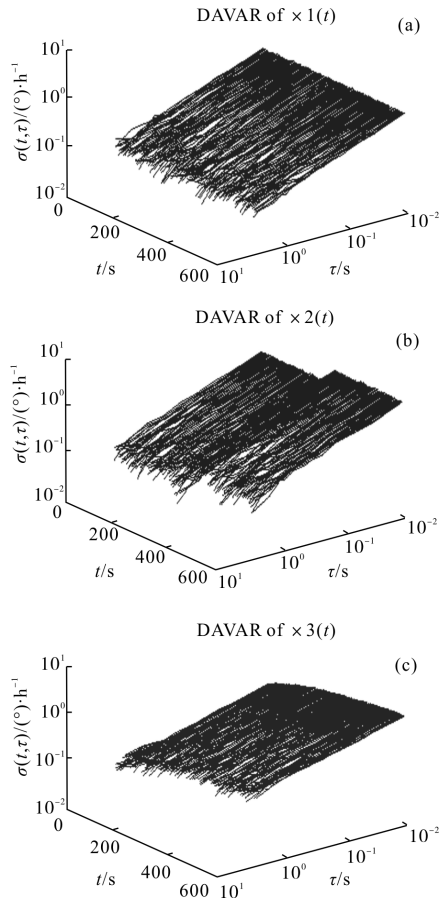


Fig.3 Three simulate data corresponding DAVAR

Studies have shown that angle random walk in FOG random error originates white noise^[9,12]. The White noise in FOG directly affects the angle random walk coefficient. In the process of calculating DADEV, the random walk coefficient can be obtained in every analysis time epoch, and then display them in chronological order in a two-dimensional graph as shown in Fig.4. Random walk coefficient of $x_1(t)$ swing nearby a constant factor while random walk coefficient of $x_2(t)$ has a step jump in the middle of signal and random walk coefficient of $x_3(t)$ increases linearly with time. The simulation results show that DAVAR not only determine the various random drift, but also can track and describe the non-stationary of time-varying signal. They fully prove the validity,

effectiveness and practicality of DAVAR.

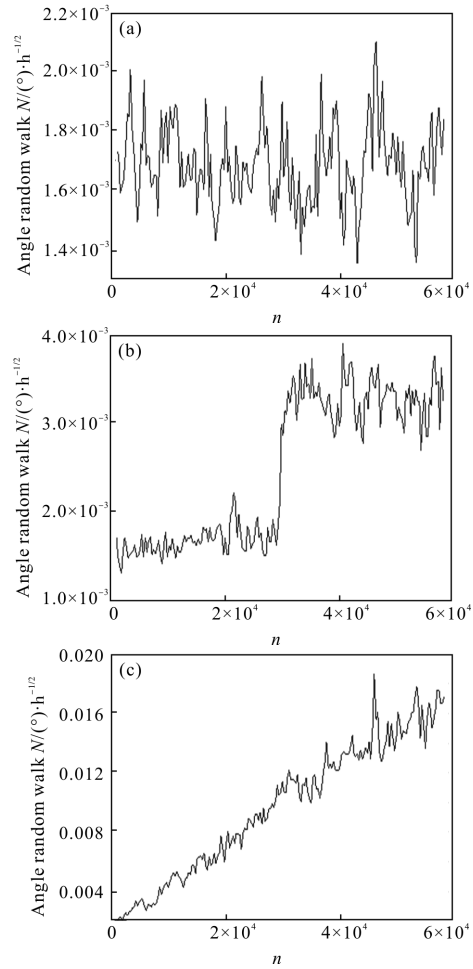


Fig.4 Simulated data corresponding angle random walk

3.2 Experimental results

3.2.1 Preheating experiment in static

To further demonstrate the validity of DAVAR, preheating experiment were done using the nominal accuracy of $0.01(^{\circ})/h$ FOG. Under the condition of room temperature $25^{\circ}C$, place a biaxial FOG system on a two axis turntable and make X, Y axis horizontal fixed FOG position. The sampling period was 10 ms and acquisition time was 11 787 s. In Fig.5, the original random drift signal $y(t)$ of FOG is shown.

The FOG is undergoing a preheating test which results in a highly nonstationary time series. As a matter of fact, $y(t)$ shows several outliers, especially at the beginning, and mean value changes with time, sometimes in an abrupt way, as happens for example around $t=11 \times 10^3$ s. We expect also the FOG stability

to be a function of time.

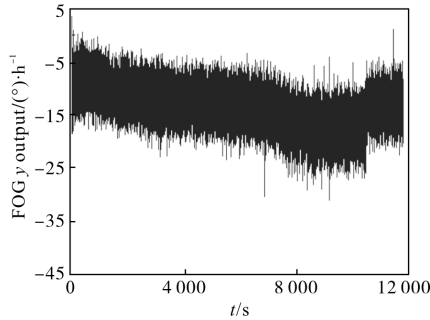


Fig.5 FOG random drift signal at static test

In Fig.6, we show the Allan deviation $\sigma_y(\tau)$ of the FOG data. The non-stationaries are not visible from this picture, which looks like the stability of a typical FOG with two mixed behavior. Because there are mainly two kinds of slope $-1/2(0.01-1\text{ s})$ and $1/2$ (more than 10 s) in Allan deviation curve.

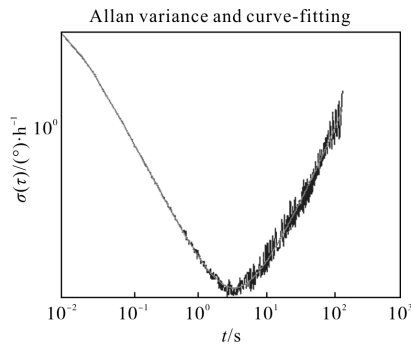


Fig.6 Allan deviation of $y(t)$

In Fig.7 we represent DADEV $\sigma_y(t, \tau)$ of the FOG data which obtained with rectangular window whose length is $L=900$ and step length is $L_0=500$. The picture gives the feeling of a FOG whose behavior is highly non-stationary. It can be seen that many localized events are due both to the outliers and to the abrupt variations. At the beginning of the data, there are some prominently jump Allan deviation curves and at $n=11 \times 10^4$ point there is a big gap, indicating that a large amplitude changes happened. Therefore DAVAR could clearly capture the signal changes. In Fig.8, we show the movement of each noise coefficient in the FOG. As expected, at the beginning and $n=11 \times 10^4$ every kinds noise coefficients have a big change, especially at $n=11 \times 10^4$ there is a peak value.

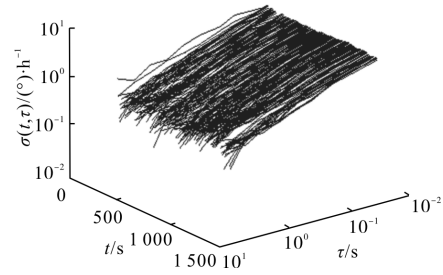


Fig.7 DAVAR analysis result of static test data for FOG

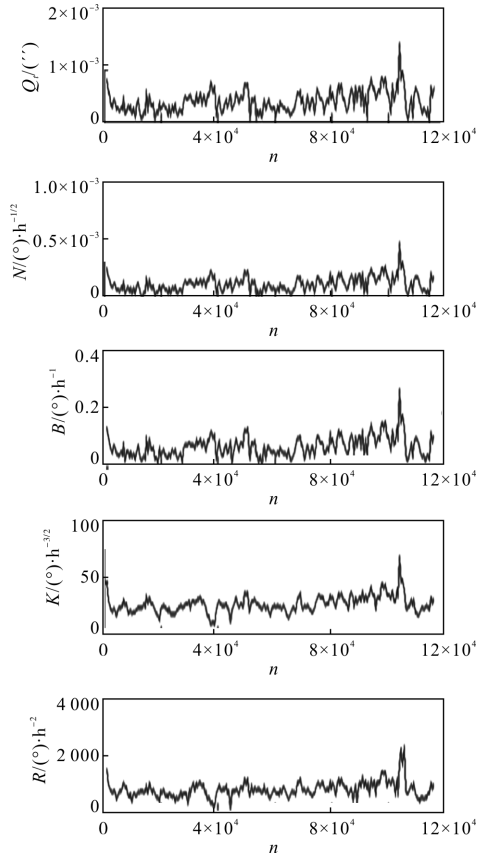


Fig.8 Change process of each noise coefficient

According to the results of DAVAR, FOG output has big fluctuations at the beginning of preheating time; it can be speculated that FOG performance is not stable in the preheating time. Consequently, we should further improve the quick start-up performance of FOG or FOG should be preheating for a longer time in order to work normally. The reason why there are outliers among the data may because human disturbance during the test, so the error messages should be pretreated. When FOG data has a mutation at $n = 11 \times 10^4$, after carefully back-check the

experiment process, we obtained that the temperature of FOG increased slowly among the test, at $n=11 \times 10^4$, the FOG temperature reached $42\text{ }^\circ\text{C}$. Because of FOG's the temperature control module has some problems leading to its output current jump and FOG output jump along with it. So it can be concluded that the temperature control module should be improved. Experiment results further prove that DAVAR is a more comprehensive, more effective and more useful tool for judging FOG performance.

3.2 Oscillate experiment

Vibration will greatly influence the performance of the FOG. In order to verify that DAVAR can reflect the dynamic changes in the performance of FOG, this paper did the vibration test with a FOG IMU. At the room temperature, Y axis gyro was put on random vibration whose average was 0 and variance is 3.7 g. The sampling period was 10 ms and acquisition time was 3005.63 s. Acquisition FOG output is shown in Fig.8.

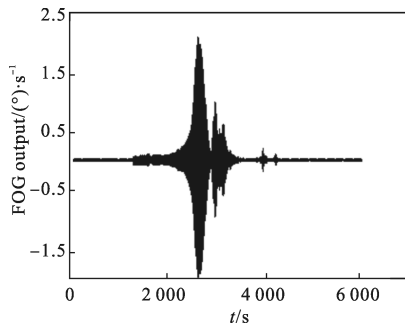


Fig.8 FOG output under random vibration

In Fig.9, DADEV of the FOG vibration data is represented which obtained with rectangular window whose length is $L=90\ 000$ and step length is $L_0=3\ 000$. The noise coefficients of two-dimensional display are shown in Fig.10.

It can be seen that the five kinds of noise coefficients value are all in low level and small change amplitude which prove that they are all in the stationary state. Thereinto the quantization noise (Q) is almost $0''$. Under the condition of vibration, all kinds of noise have a big change. The quantization noise (Q) is always in a high level about $5''$ while

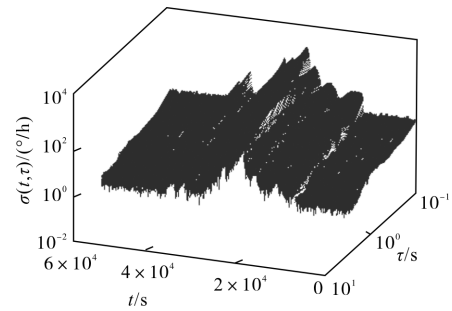


Fig.9 DADEV of FOG vibration data

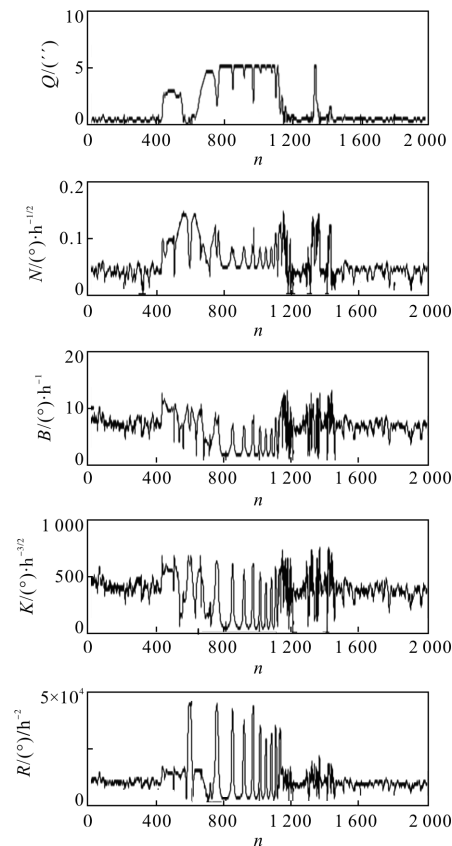


Fig.10 Change process of each noise coefficient

other kinds of noise present periodical oscillate, especially the rate random walk (R) and the rate slope (K) have a large amplitude. Though short truncation widow bring to fitting error, it can be inferred that the two kinds of noise are influenced by vibration more seriously. After the vibration stopped, all kinds of noise coefficients are back to the level before vibration gradually. It can be concluded that FOG could undertake vibration at least 3.7 g.

4 Conclusions

FOG is influenced by environmental factors such

as temperature, humidity, radiation, a sudden power failure, the device aging and other factors which leading its static data to emerge non-stationary characteristics. Because classical Allan variance could not characterize the non-stationary, we raised DAVAR to analyze the FOG data. Using simulated data and experimental data to verify the effectiveness and usefulness of DAVAR. On conclusions, DAVAR not only can determine the coefficients of FOG random error, but also can describe the non-stationary of FOG. What's more, the quantitative description of each noise in a two-dimensional graph is also realized which can show noise changes with time.

In the study of DAVAR, calculation speed of DAVAR become very slowly in the case of large amount of data was found. In future work, DAVAR algorithm should be improved to raise computing speed. What's more, to track fast variations in time, it needs a short window; while to keep the variance of the estimate low, it needs a long window. This is an evident tradeoff and hence the influence of window length on the confidence of DAVAR should be studied. Another issue is implementation of a real-time DAVAR estimator. Now DAVAR just can analyze the off-line data. In many applications, such as navigation, a real-time evaluation of the DAVAR may be necessary.

References:

- [1] Lefevre H C. Zhang Guicai, Wang Wei. Fiber Optic Gyroscope [M]. Beijing: National Defence Industry Press, 2002. (in Chinese)
- [2] Stein S R. The Allan variance—challenges and opportunities [J]. *IEEE Transactions on Ultrasonics, Ferroelectrics, and Frequency Control*, 2010, 57(3): 540–547.
- [3] Lorenzo Galleani, Patrizia Tavella. Tracking nonstationarities in clock noises using the dynamic Allan variance [C]//SPIE, Proc Joint FCS–PTTI Meeting, 2005: 392–396.
- [4] Lorenzo Galleani, Patrizia Tavella. The Dynamic Allan variance [J]. *IEEE Transactions on Ultrasonics, Ferroelectrics, and Frequency Control*, 2009, 56(3): 540–547.
- [5] Lorenzo Galleani, Patrizia Tavella. Fast computation of the dynamic Allan variance [C]//SPIE, Proc IEEE FCS–EFTF, 2009: 685–687.
- [6] Lorenzo Galleani. The dynamic Allan variance II: A fast computational algorithm [J]. *IEEE Transactions on Ultrasonics, Ferroelectrics, and Frequency Control*, 2009, 57(1): 182–188.
- [7] Lorenzo Galleani. The dynamic Allan variance III: confidence and detection surfaces [J]. *IEEE Transactions on Ultrasonics, Ferroelectrics, and Frequency Control*, 2011, 58(8): 1550–1558.
- [8] Wei Guo, Long Xingwu. Research on Stochastic errors of dithered ring laser gyroscope based on dynamic allan variance [J]. *Chinese Journal of Lasers*, 2010, 37(12): 2975–2979. (in Chinese)
- [9] Li Ying, Chen Xinglin, Song Shenmin. Dynamic Allan variance analysis for the drift error of fiber optical gyroscope [J]. *Journal of Optoelectronics·Laser*, 2008, 19(2): 183–186. (in Chinese)
- [10] Li Xuyou, Zhang Na. Analysis of dynamic characteristics of a fiber optic gyroscope based on dynamic Allan variance [J]. *Journal of Harbin Engineering University*, 2011, 32(2): 183–187. (in Chinese)
- [11] Zhang Na, Li Xuyou. Research on theoretical improvement of dynamic Allan variance and its application [J]. *Acta Optica Sinica*, 2011, 31(11): 1–6. (in Chinese)
- [12] Xiong Kai, Lei Yongjun, Zeng Haibo. Modeling and simulation of fiber optic gyros based on allan variance method [J]. *Aerospace Control and Application*, 2010, 36(3): 7–13. (in Chinese)